Conference paper

Claudio Mortier, Romain Bourd, Guilhem Godeau, Frédéric Guittard and Thierry Darmanin*

Superhydrophobic and superoleophobic poly(3,4-ethylenedioxypyrrole) polymers synthesized using the Staudinger-Vilarrasa reaction

DOI 10.1515/pac-2017-0206

Abstract: Vegetal and animal reigns offer many examples of surfaces with surprising and interesting wetting properties. As example, springtails present superoleophobic properties allowing to live in soil and *Lotus* leaves show self-cleaning ability even under rainfalls. Indeed, it is known that self-cleaning properties can help to remove dust and particles during rainfalls and as a consequence to clean the surface. The bioinspiration of these surface properties is of a real interest for industrial applications in the nanotechnology field such as photovoltaic systems or anti corrosive material. Here, we use a strategy based on electropolymerization to obtain these properties. The Staudinger-Vilarrasa reaction is used to prepare innovative 3,4-ethylenedioxypyrrole (EDOP) monomers with fluorinated chains. Using C_6F_{13} or C_8F_{17} chains, the polymer surfaces formed after electrodeposition show superhydrophobic and superoleophobic features. Here we study the surface wettability depending on the surface energy (based on the perfluorinated chain length), the surface roughness and morphology.

Keywords: bioinspiration; click chemistry; electrochemistry; NICE-2016; superhydrophobicity; superoleophobicity.

Introduction

The control of surface wettability is a hot field of research in different fields including self-cleaning surfaces, biofouling paints, adhesives and separation membranes [1–4]. Scientific and industrial communities have highly searched in order to better understand the various wetting behaviors. Some equations are now very often used. The Young Dupré equation gives the apparent contact angle of a smooth surface (θ^Y) at the triple point [5]. This θ^Y is depending on three surface tensions: solid-vapor γ_{SV} or material surface energy, solid-liquid γ_{SL} and liquid-vapor γ_{LV} or liquid surface tension. The reaction is $\cos\theta^Y = (\gamma_{SV} - \gamma_{SL})/\gamma_{LV}$. For rough surfaces, two other equations are very often used: the Wenzel and the Cassie – Baxter equations [6, 7]. These models can explain highly hydrophobic and highly hydrophilic features. For example, the Wenzel

Article note: A collection of invited papers based on presentations at the 3rd International Conference on Bioinspired and Biobased Chemistry and Materials: Nature Inspires Creativity Engineers (NICE-2016), Nice, France, 16–19 October 2016.

***Corresponding author: Thierry Darmanin,** Université Côte d'Azur, NICE Lab, IMREDD, 61-63 Av. Simon Veil, 06200 Nice, France, e-mail: thierry.darmanin@unice.fr
Claudio Mortier, Romain Bourd, Guilhem Godeau and Frédéric Guittard: Université Côte d'Azur, NICE Lab, IMREDD, 61-63 Av. Simon Veil, 06200 Nice, France

equations [6] allows to better understand highly hydrophobic surfaces with high adhesion properties while the Cassie – Baxter equation [7] surfaces with low adhesion (superhydrophobicity) [8] even if intermediate states also exist (petal effect or parahydrophobicity) [9, 10]. Based on these equations and observations in nature, [11–15] it is possible to distinguish parameters of particular interest to reproduce these features. In particular, the surface energy (γ_{SV}) and the surface structures are essential parameters. The question now is: "how to control both parameters?". Many answers have been given to this question by research groups around the world and many processes have been developed to control these parameters [16–19]. Among them, the conductive polymer electrodeposition or electropolymerization is of particular interest [20, 21] This strategy is highly efficient to prepare, very quickly and with a reasonable cost, surfaces with various wettability properties such as superhydrophobic, parahydrophobic and even superoleophobic properties (surface repelling oils). By playing on the intrinsic hydrophobic feature of the monomer and a substituent, which can be easily grafted on the monomer, and on the electropolymerization parameters, it is possible to finely tune the final properties of the surface. 3,4-ethylenedioxypyrrole (EDOP) is an exception monomer for these applications [22–24]. Even if, to date, the monomer is extremely complex to synthesize, [25–28] the presence of the ethylenedioxybrigde on pyrrole allows to have monomers with ultra-low oxidation potentials (below –1 V vs. SCE) while the nitrogen can be easily used to graft various substituents. Moreover, it was shown the possibility to obtain superoleophobic properties due to the presence of both microstructures and nanoporosities/nanostructures [22].

Here, in the aim to use the Staudinger-Vilarrasa reaction to graft various substituents with amide groups, [29–31] an original EDOP monomer with an azido group was first synthesized (Scheme 1). Then, different fluorinated chains (C_4F_9, C_6F_{13} and C_8F_{17}) were introduced.

Experimental section

3,4-ethylenedioxypyrrole (EDOP) was synthesized in eight steps from iminodiacetic acid as shown in Scheme 2 [28]. Separately, 1-azido-10-bromodecane was synthesized with 1,10-dibromodecane and sodium azide. On the core of EDOP, the alkyl spacer with an azide group was added by nucleophilic substitution. Then, by a Staudinger-Vilarrasa reaction, [29] different fluorinated chains were obtained (Scheme 3).

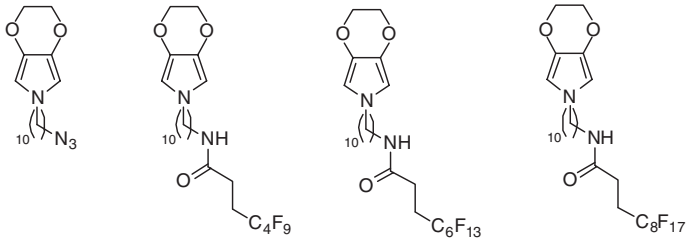

Scheme 1: Original monomers obtained and studied in this work.

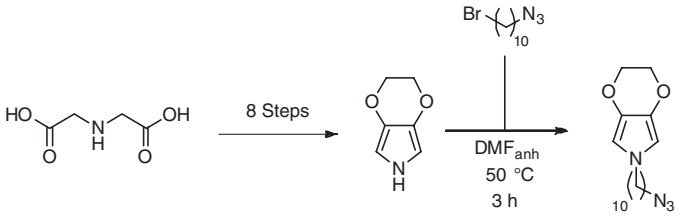

Scheme 2: Synthesis of precursor monomer.

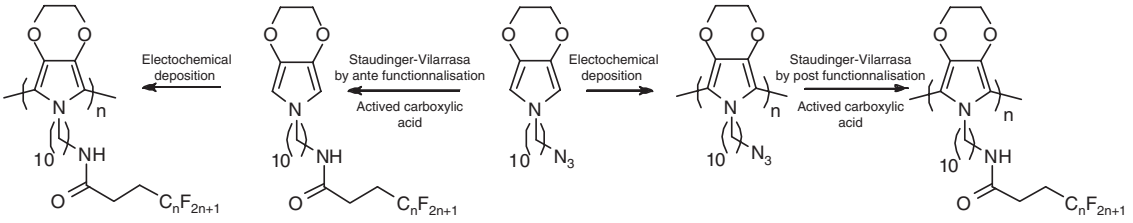

Scheme 3: Two synthesis strategies for drive to hybrid functionalized polymers.

Synthesis of 1-azido-10-bromodecane

To 50 mL of N,N-dimethylformamide (DMF), were added 1,10-dibromodecane (16 mmol, 1 equiv.) and sodium azide (16 mmol, 1 equiv.). The mixture was stirred and heated at 95 °C for 1 day. Then, the solvent was evaporated and purified by column chromatography using silica gel and cyclohexane as eluent for obtained the 1-azido-10-bromodecane.

1-azido-10-bromodecane

Yield 33 %; colourless liquid; δH(200 MHz, $CDCl_3$): 3.41 (2 H, t, $^3J_{HH}$ = 6.8 Hz), 3.26 (2 H, t, $^3J_{HH}$ = 6.8 Hz), 1.81 (2 H, q, $^3J_{HH}$ = 6.6 Hz), 1.56 (2 H, q, $^3J_{HH}$ = 6.6 Hz), 1.3 (12 H, m).

Synthesis of the precursor monomer by nucleophilic substitution of 3,4-ethylenedioxypyrrole

To 20 mL of anhydrous N,N-dimethylformamide, were added 3,4-ethylenedioxypyrrole (3,3 mmol, 1 equiv.) and potassium hydroxide (6,7 mmol, 2 equiv.). The mixture was stirred and heated during 30 min at 45 °C. Then, 1-azido-10-bromodecane (5 mmol, 1,5 equiv.) was added droplet by droplet to the mixture diluted in 10 mL of anhydrous N,N-dimethylformamide. The solution was stirred and heated at 45 °C for 3 h. Then, The mixture was evaporated and purified by column chromatography using gel silica and cyclohexane/ethyl acetate as eluent to obtain the precursor monomer 6-(10-azidodecyl)-3,6-dihydro-2H-[1,4]dioxino[2,3-c] pyrrole (EDOP-C_{10}-N_3).

6-(10-azidodecyl)-3,6-dihydro-2H-[1,4]dioxino[2,3-c]pyrrole (EDOP-C_{10}-N_3)

Yield 30 %; orange liquid; δH(200 MHz, $CDCl_3$): 6.05 (2 H, s), 4.17 (4 H, s), 3.63 (2 H, t, $^3J_{HH}$ = 7 Hz), 3.25 (2 H, t, $^3J_{HH}$ = 6.8 Hz), 1.59 (4 H, m), 1.26 (12 H, m); δC(200 MHz, $CDCl_3$): 131.61, 100.95, 65.83, 51.45, 50.19, 31.30, 29.43, 29.34, 29.23, 28.79, 26.66, 26.64.

Synthesis of the monomers by *Staudinger-Vilarrasa* reaction

To 20 mL of anhydrous tetrahydrofuran (THF), were added 4-dimethylaminopyridine (0,72 mmol, 2,2 equiv.), 1-ethyl-3-(3-dimethylaminopropyl)carbodiimide (0,59 mmol, 1,8 equiv.) and 4,4,5,5,6,6,7,7,7-nonafluoroheptanoic acid or 4,4,5,5,6,6,7,7,8,8,9,9,9-tridecafluorononanoic acid or 4,4,5,5,6,6,7,7,8,8,9,9,10,10,11,11,11-heptadecafluoroundecanoic acid (0,5 mmol, 1,5 equiv.). The mixture was stirred at room temperature during 30 min to activate the carboxylic acid. Then, EDOP-C_{10}-N_3 was added diluted in 10 mL of anhydrous THF droplet by droplet. The solution was stirred at room temperature during 3 h. After the solution was purified by column chromatography using gel silica and a melt of cyclohexane/ethyl acetate as eluent.

N-(10-(2H-[1,4]dioxino[2,3-c]pyrrol-6(3H)-yl)decyl)-4,4,5,5,6,6,7,7,7-nonafluoroheptanamide (EDOP-C_{10}-NHCO-EC_4F_9)

Yield 55 %; white powder; δH(200 MHz, $CDCl_3$): 6.05 (2 H, s), 5.54 (1 H, t), 4.17 (4 H, s), 3.63 (2 H, t, $^3J_{HH}$ = 6.8 Hz), 3.27 (2 H, t, $^3J_{HH}$ = 6.6 Hz), 2.48 (4 H, m), 1.65 (2 H, m), 1.51 (2 H, m), 1.25 (12 H, m); δC(200 MHz, $CDCl_3$): 169.58, 131.61, 100.97, 65.83, 50.20, 39.82, 31.28, 29.50, 29.33, 29.16, 29.11, 27.16, 27.09, 26.80 δF(200 MHz, $CDCl_3$): –81.06 (3 F, m), –114.87 (2 F, m), –124.49 (2 F, m), –126.05 (2 F, m).

N-(10-(2H-[1,4]dioxino[2,3-c]pyrrol-6(3H)-yl)decyl)-4,4,5,5,6,6,7,7,8,8,9,9,9-tridecafluorononanamide (EDOP-C_{10}-NHCO-EC_6F_{13})

Yield 54 %; yellow powder; δH(200 MHz, $CDCl_3$): 5.97 (2 H, s), 5.47 (1 H, t), 4.11 (4 H, s), 3.57 (2 H, t, $^3J_{HH}$ = 7 Hz), 3.20 (2 H, t, $^3J_{HH}$ = 6.8 Hz), 2.41 (4 H, m), 1.59 (2 H, m), 1.43 (2 H, m), 1.18 (12 H, m); δC(200 MHz, $CDCl_3$): 169.60, 131.62, 100.97, 65.84, 50.20, 39.83, 31.28, 29.51, 29.33, 29.16, 29.11, 27.16, 27.09, 26.80; δF(200 MHz, $CDCl_3$): –80.79 (3 F, m), –114.66 (2 F, m), –121.94 (2 F, m), –122.90 (2 F, m), –123.57 (2 F, m), –126.20 (2 F, m).

N-(10-(2H-[1,4]dioxino[2,3-c]pyrrol-6(3H)-yl)decyl)-4,4,5,5,6,6,7,7,8,8,9,9,10,10,11,11,11-heptadecafluoroundecanamide (EDOP-C_{10}-NHCO-EC_8F_{17})

Yield 40 %; yellow powder; δH(200 MHz, $CDCl_3$): 6.05 (2 H, s), 5.54 (1 H, t), 4.18 (4 H, s), 3.63 (2 H, t, $^3J_{HH}$ = 7 Hz), 3.27 (2 H, t, $^3J_{HH}$ = 6.8 Hz), 2.47 (4 H, m), 1.64 (2 H, m), 1.42 (2 H, m), 1.25 (12 H, m); δC(200 MHz, $CDCl_3$): 169.59, 131.60, 100.96, 65.83, 50.18, 39.82, 31.27, 29.49, 29.32, 29.15, 29.10, 26.79, 26.59; δF(200 MHz, $CDCl_3$): –80.76 (3 F, m), –114.66 (2 F, m), –121.82 (6 F, m), –122.67 (2 F, m), –123.51 (2 F, m), –126.11 (2 F, m).

Electrochemical conditions

An Autolab potentiostat purchased from Metrohm was used for the electrodeposition experiments. The connection was realized *via* a three-electrode system. A platinum tip was used as working electrode for cyclic voltammetry experiments, a carbon rod as counter-electrode while a saturated calomel electrode (SCE) was used as reference electrode. For the surface characterization, the polymers were electrodeposited on gold plates purchased from Neyco and consisting in a deposition of chromium (20 nm) and gold (150 nm) on silicon wafer. In a glass cell, connected to the potentiostat with the three-electrode system, 10 mL of anhydrous acetonitrile containing 0.1 M of electrolyte (tetrabutylammonium perchlorate) and 0.01 M of monomer were introduced under argon. First, the monomer oxidation potential (0.86–1.08 V vs. SCE following the alkyl chain length of the monomer) was determined by cyclic voltammetry with the platinum tip as working electrode. Multiple potential scans were performed to study the polymer growth and to determine the polymer oxidation and reduction potentials. Then, polymer films were electrodeposited by cyclic voltammetry (CV) or at imposed potential (IP) on larger gold plates. Six depositions by imposed potential were performed for each monomer at several deposition charge during the experiments: 12.5, 25, 50, 100, 200, 400 mC cm^{-2}. Depositions at 1 mC cm^{-2} were also performed to prepared smooth polymer films.

Surface characterization

Polymers were characterized by goniometry, scanning electron microscopy (SEM) and optical profilometry. The SEM images were recorded using a 6700F microscope (JEOL) in the CCMA (Centre Commun de Microscopie appliquée, Univ. Nice Sophia Antipolis). The mean arithmetic (Ra) and quadratic (Rq) roughness were

determined using a Wyko NT 1100 optical microscope (Bruker) the objective 50×, and the field of view (FOV) 0.5×. VSI mode was used for smooth surfaces and PSI mode was used for very rough surfaces. The apparent contact angles (θ) were measured using a DSA30 goniometer (Krüss) by taking the tangent at the triple point contact line with a droplet of 2 µL. For the dynamic contact angles, a 4 µL water droplet was put on the substrate, and the substrate was inclined until the droplet moves. The advanced and receding contact angles are taken just before the droplet moving. The maximum inclination angle is called sliding angle (α). If the droplet does not move even for $\alpha > 90°$, the hysteresis is extremely high and the substrate is called sticky (parahydrophobic) [10]. The surface free energy (γ_{SV}) of the smooth surfaces and its dispersive (γ^{D}_{SV}) and polar (γ^{P}_{SV}) parts were determined using the Owens–Wendt equation: $\gamma_{LV}(1+\cos\theta) = 2(\gamma^{D}_{LV}.\gamma^{D}_{SV})^{1/2} + 2(\gamma^{P}_{LV}.\gamma^{P}_{SV})^{1/2}$. Using three different liquids (water, diiodomethane, hexadecane, for which γ_{LV}, γ^{D}_{LV} and γ^{P}_{LV} are known, γ^{D}_{SV} and γ^{P}_{SV} can be calculated by drawing the function $y = ax + b$ where $y = \gamma_{LV}(1+\cos\theta)/2(\gamma^{D}_{LV})^{1/2}$ and $x = (\gamma^{P}_{LV})^{1/2}/(\gamma^{D}_{LV})^{1/2}$. Then, $\gamma^{D}_{SV} = b^2$ and $\gamma^{P}_{SV} = a^2$ are determined. In our case, γ^{D}_{SV} and γ^{P}_{SV} were directly obtained using the software "Drop Shape Analysis" of our goniometer.

Results and discussion

Deposition experiments

The electropolymerization experiments were performed in anhydrous acetonitrile containing 0.01 M monomer and 0.1 M tetrabutylammonium perchlorate (Bu_4NClO_4) used as electrolyte. First, it was necessary to determine the monomer oxidation potential (E^{ox}_m) by cyclic voltammetry to know the intervals of tension where the monomer is reactive (oxidized). The measurements of the monomer oxidation potential of each monomer (E^{ox}_m), also called sometimes reduction potentials of the monomer oxidation, [32] are reported on Table 1. The potential is close the same for all the polymer which means that the length of the fluorinated chains has not a significant effect on the oxidation of the monomer because of the presence of the very long decyl spacer.

In order to study the growth of the polymers, 10 scans of cyclic voltammetry were performed between –1 and E^{ox}_m on the platinum working electrode. The cyclic voltammograms are shown in Fig. 1. The voltammograms of each polymer shows very intense oxidation and reduction polymer curves between a range of 0.23 V and the E^{ox}_m with a perfect superposition after each scan indicating that the polymerization proceeds perfectly and that the amount of electrodeposited polymer is quite constant after each scan. More precisely, two oxidation and reduction peaks are observed in the voltammograms. As it was done in first experiments, the peak at around 0.90 V during the forward scans corresponds to the oxidation of the monomer. The other peaks observed during the forward scans correspond to the polymer oxidations and the other peaks observed during the back scans corresponds to the polymer reductions. Usually, the size, the position and electronic effect of the substituent can affect the polymer growth. Here, the position of the peaks is close the same for all polymers indicating that the decyl spacer allows to reduce the steric hindrance induce by the azide or the fluorinated chains. This is in agreement with previous works showing that due to very high van der Waals interactions, a decyl spacer is suitable to functionalize EDOP monomers on the nitrogen [33]. It was also shown in the literature that the presence of the second peak, [21] which seems to be due to a complex doping process, is important in the formation of surface nanoporosities/nanostructuration. Here, the second peak is extremely low with azide groups but extremely intense with the fluorinated chains.

Table 1: Monomer oxidation potentials (vs. SCE).

	PEDOP-C_{10}-NHCO-EC_8F_{17}	PEDOP-C_{10}-NHCO-EC_6F_{13}	PEDOP-C_{10}-NHCO-EC_4F_9	PEDOP-C_{10}-N_3
E^{ox}_m (V)	0.90	0.88	0.90	0.90

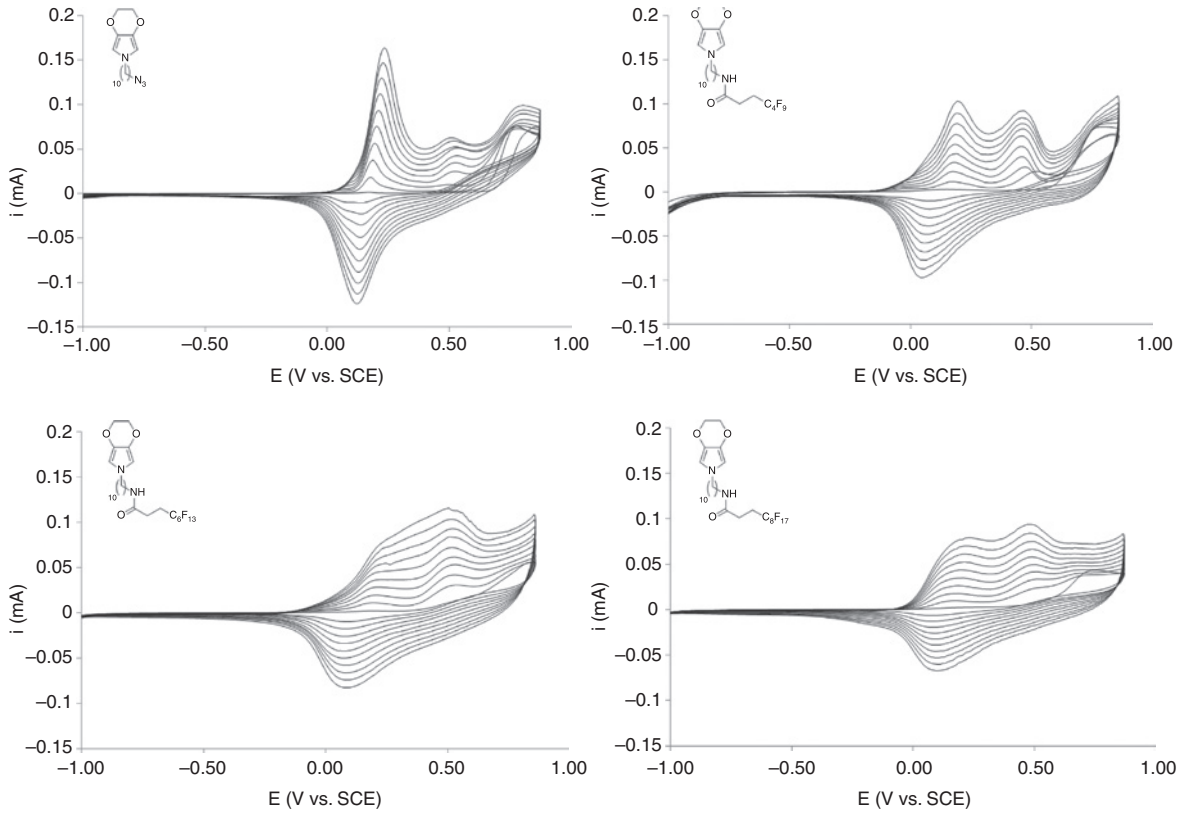

Fig. 1: Ten scans of cyclic voltammetry of different monomers. Scan rate 20 mV.s^{-1}.

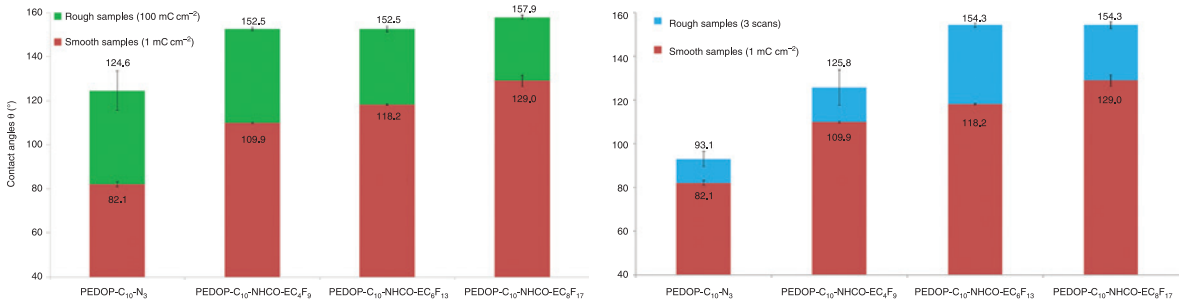

Fig. 2: Graphic of the contact angle with water of rough polymers deposited by imposed potential at 100 mC cm^{-2} (left) and CV with 3 scans of deposition (right) compared to the smooth polymers.

Then in order to study the wettability of this polymers, different samples were performed on gold working substrates by cyclic voltammetry with 1, 3 and 5 deposition scans and at imposed potential with different deposition charges: 1 mC cm^{-2} for the smooth samples (with a roughness <10 nm) and 12.5, 25, 50, 100, 200 and 400 mC cm^{-2} for the rough samples. The depositions at imposed potential lead to conductive polymers in the oxidized state while by cyclic voltammetry the polymers are obtained in the reduced state.

Surface wettability and surface morphology

In order to evaluate the wetting behavior of the PEDOP derivatives, different probe liquids were studied (water, diiodomethane and hexadecane) to better characterize the surface hydrophocity and oleophobicity.

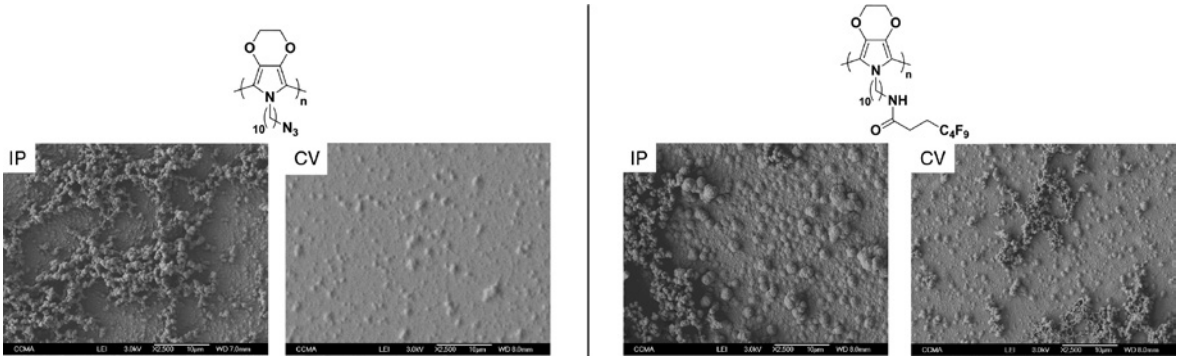

Fig. 3: SEM images of PEDOP-C_{10}-N_3 and PEDOP-C_{10}-NHCO-EC_4F_9 deposited by imposed potential at 100 mC cm^{-2} (left) and CV with 3 scans of deposition (right).

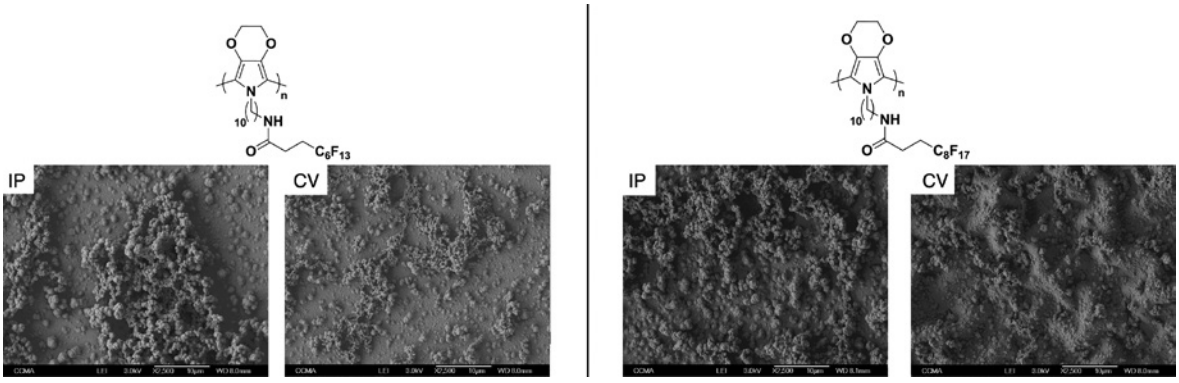

Fig. 4: SEM images of PEDOP-C_{10}-NHCO-EC_6F_{13} and PEDOP-C_{10}-NHCO-EC_8F_{17} deposited by imposed potential at 100 mC cm^{-2} (left) and CV with 3 scans of deposition (right).

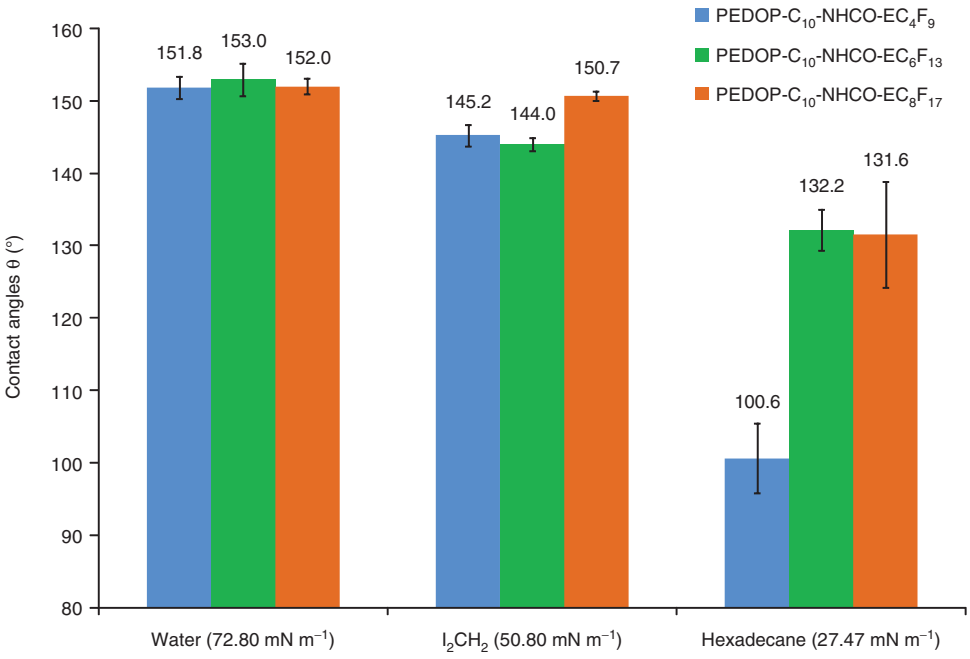

Fig. 5: Wettability of PEDOP-C_{10}-NHCO-EC_8F_{17}, PEDOP-C_{10}-NHCO-EC_6F_{13}, PEDOP-C_{10}-NHCO-EC_4F_9 deposited at 200 mC cm^{-2} by imposed potential with different liquid.

Table 2: θ_w ($Qs = 200$ mC · cm^{-2}) and θ^{γ}_w ($Qs = 1$ mC · cm^{-2}) and dynamic contact angle.

Polymers	θ_w [deg]	θ^{γ}_w [deg]	ΔH [deg]	α [deg]	Adhesion behavior	Appellation
PEDOP-C_{10}-NHCO-EC_4F_9	151.8	109.9	103.0	28.0	Sticky	Parahydrophobic
PEDOP-C_{10}-NHCO-EC_6F_{13}	152.9	118.2	3.1	8.9	Self-sliding	Superhydrophobic
PEDOP-C_{10}-NHCO-EC_8F_{17}	152.0	129.0	1.1	5.4	Self-sliding	Superhydrophobic

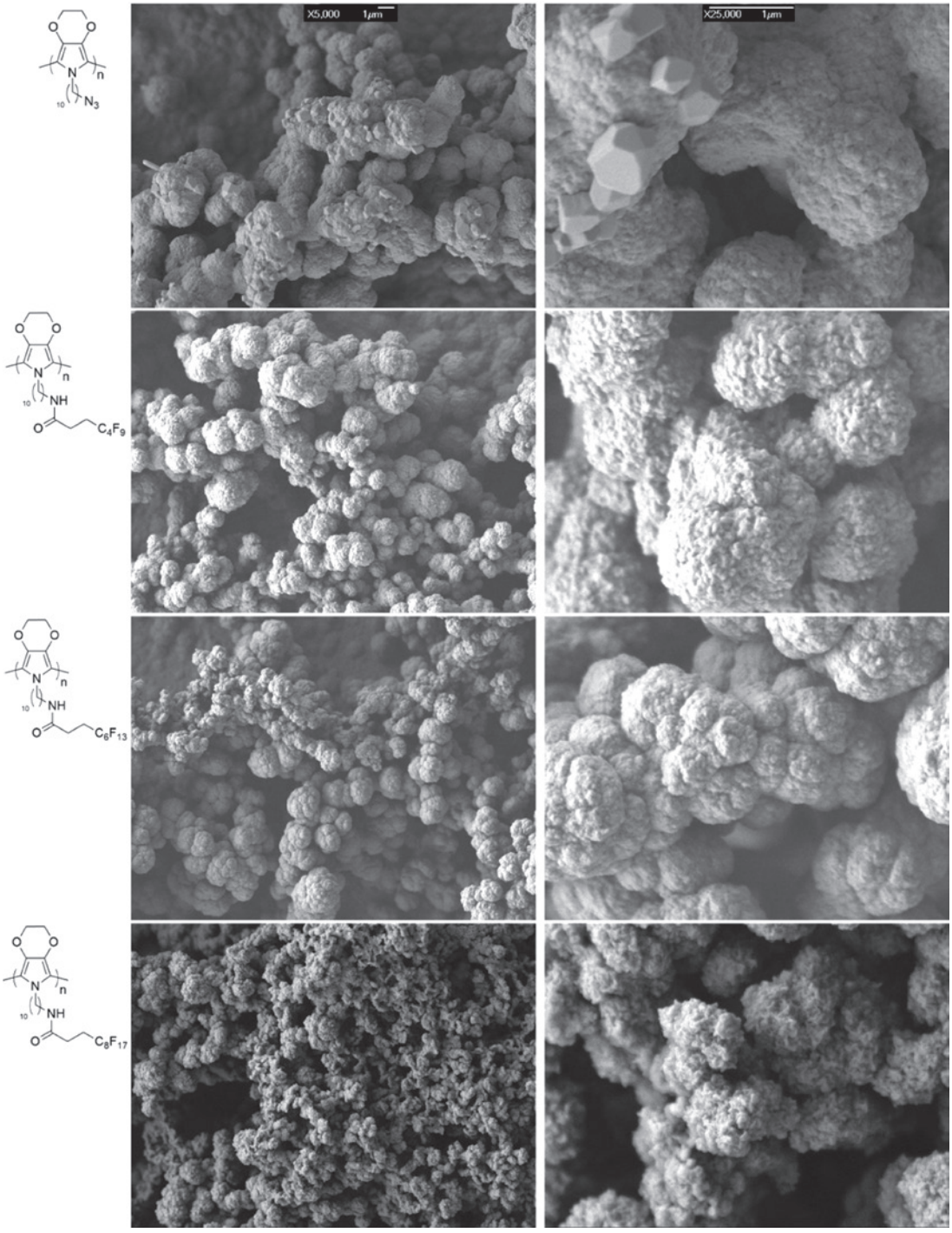

Fig. 6: SEM images of polymers deposited by imposed potential ($Qs = 200$ mC · cm^{-2}) with a magnification at ×5000 (left side) and ×25 000 (right side).

Table 3: Wettability and roughness parameters for smooth polymers ($Qs = 1\ mC \cdot cm^{-2}$) obtained in Bu_4NClO_4 and measurements of their surface free energies.

Polymers	R_a [nm]	R_q [nm]	θ^Y_w [deg]	θ^Y_{diiodo} [deg]	$\theta^Y_{hexadecane}$ [deg]	γ_{sv} [mN·m^{-1}]	γ^D_{sv} [mN·m^{-1}]	γ^P_{sv} [mN·m^{-1}]
PEDOP-C_{10}-NHCO-EC_8F_{17}	12.6	20.5	129.0	100.5	77.3	9.64	9.63	0.01
PEDOP-C_{10}-NHCO-EC_6F_{13}	10.2	14.1	118.2	93.7	67.9	11.22	10.99	0.23
PEDOP-C_{10}-NHCO-EC_4F_9	9.6	12.1	109.9	85.3	63.5	15.03	14.09	0.94

The comparison between rough and smooth polymers shows the impact of the surface roughness on the wettability. First, at imposed potential (100 mC cm^{-2}), the contact angles are higher than by cyclic voltammetry (3 scans) (Fig. 2). As expected, the higher properties were obtained with C_8F_{17}, for which superhydrophobic and superoleophobic properties are obtained.

Indeed, it was observed higher surface structuration at imposed potential than by cyclic voltammetry (Figs. 3 and 4), especially for PEDOP-C_{10}-N_3, explained the differences measured on these surfaces.

The largest contact angles were obtained at imposed potential and using a deposition charge of 200 mC·cm^{-2} (Fig. 5 and Table 2), for which superhydrophobic and superoleophobic properties are obtained with C_8F_{17}, and C_6F_{13}. These two polymers also displayed ultra-low water adhesion compared to with C_4F_9, which is parahydrophobic.

SEM images at higher magnification (Fig. 6) show a relatively similar surface morphology with both micro and nanostructures. Only PEDOP-C_{10}-NHCO-EC_8F_{17} is more nanostructured than the other polymers, explaining the exceptional results obtained with this polymer. Hence, PEDOP-C_{10}-NHCO-EC_4F_9 is less hydrophobic and oleophobic especially because the fluorinated chain is shorter and as a consequence the polymer surface energy is higher.

Discussion

The wettability results can be explained theoretically by the equation of Young Dupré [5] for the smooth surfaces and the equations of Wenzel, [6] Cassie – Baxter [7] for the rough surfaces. These relations are often used for understanding wettability behavior of surfaces. First, the smooth polymers are all intrinsically hydrophobic (Table 3) with a θ^Y_w between 109° and 129° for the fluorinated ones. The surface energy (γ_{SV}) and their polar (γ^P_{SV}) and apolar (γ^D_{SV}) components were also calculated using three liquid probes and using the Owens-Wendt equation. As expected, the polymer with the longest fluorinated chains (PEDOP-C_{10}-NHCO-EC_8F_{17}) is the most hydrophobic and oleophobic and has the lowest surface energy (below 10 mN/m).

For the rough substrates, the surface morphology being close for all surfaces, it is expected that their surface hydrophobicity and oleophobicity increase with the fluorinated chain length because (γ_{SV}) decreases. This is what it was observed here. The amount of air present between of liquid droplet and the rough surfaces increases also with the fluorinated chain length, which allows the possibility to obtain superhydrophobic and superoleophobic properties. Of course, the amount of air present with a water droplet is much more important than with an oil droplet because the liquid surface tension (γ_{LV}) is higher.

Other experiments

In order to do *post*-functionalization treatment with PEDOP-C_{10}-N_3 as a platform polymer, depositions of this polymers have been done at 12.5, 25, 50, 100, 200 and 400 $mC \cdot cm^{-2}$. The protocol of *post*-functionalization on substrates with azide function are described in the literature. The substrate need to be immerged during 3 h under vigorous agitation into a solution of activated fluorinated carboxylic acid with DMAP, EDC and triphenylphosphine in anhydrous THF medium. A few second after the immersion, the polymeric films of

PEDOP-C_{10}-N_3 (at any charge of deposition) dissolved in the THF medium meaning that the bonds between the film and the gold substrate are broken during this treatment.

Conclusion

On this paper, inspired by superoleophobic springtails and superhydrophobic Lotus leaves, we reproduced these surface properties. The Staudinger-Vilarrasa reaction was used to prepare novel 3,4-ethylenedioxypyrrole (EDOP) monomers with fluorinated chains. Here we study the surface wettability depending on the surface energy (as a function of the perfluorinated chain length), the surface roughness and morphology. Using C_6F_{13} or C_8F_{17} chains, the polymer surfaces show superhydrophobic and superoleophobic features due to the presence of both micro and nanostructures. Such materials could be used in various potential applications such as in anti-corrosion, oil/water separation membranes or in anti-soil textiles.

References

[1] T. Darmanin, F. Guittard. *J. Mater. Chem. A* **2**, 16319 (2014).
[2] B. Su, Y. Tian, L. Jiang. *J. Am. Chem. Soc.* **138**, 1727 (2016).
[3] A. Milionis, E. Loth, I. S. Bayer. *Adv. Colloid Interface Sci.* **229**, 57 (2016).
[4] Y. Lai, J. Huang, Z. Cui, M. Ge, K.-Q. Zhang, Z. Chen, L. Chi. *Small* **12**, 2203 (2016).
[5] T. Young. *Philos. Trans. R. Soc. Lond.* **95**, 65 (1805).
[6] R. N. Wenzel. *Ind. Eng. Chem.* **28**, 988 (1936).
[7] A. B. D. Cassie, S. Baxter. *Trans. Faraday Soc.* **40**, 546 (1944).
[8] K. Koch, B. Bhushan, W. Barthlott. *Prog. Mater. Sci.* **54**, 137 (2009).
[9] L. Feng, Y. Zhang, J. Xi, Y. Zhu, N. Wang, F. Xia, L. Jiang. *Langmuir* **24**, 4114 (2008).
[10] A. Marmur. *Soft Matter* **8**, 6867 (2012).
[11] C. R. Szczepanski, T. Darmanin, F. Guittard. *Adv. Colloid Interface Sci.* **241**, 37 (2017).
[12] R. Hensel, R. Helbig, S. Aland, H.-G. Braun, A. Voigt, C. Neinhuis, C. Werner. *Langmuir* **29**, 1100 (2013).
[13] R. Helbig, J. Nickerl, C. Neinhuis, C. Werner. *PLoS One* **6**, e25105 (2011).
[14] Z. Sun, T. Liao, K. Liu, L. Jiang, J. H. Kim, S. X. Dou. *Small* **10**, 3001 (2014).
[15] Z. Sun, T. Liao, K. Liu, L. Jiang, J. H. Kim, S. X. Dou. *Nano Res.* **6**, 726 (2013).
[16] J. Yong, F. Chen, Q. Yang, X. Hou. *Soft Matter* **11**, 8897 (2015).
[17] F. Li, Y. Tu, J. Hu, H. Zou, G. Liu, S. Lin, G. Yang, S. Hu, L. Miao, Y. Mo. *Polym. Chem.* **6**, 6746 (2015).
[18] A. P. Kharitonov, G. V. Simbirtseva, V. G. Nazarov, V. P. Stolyarov, M. Dubois, J. Peyroux. *Prog. Org. Coat.* **88**, 127 (2015).
[19] C. R. Szczepanski, I. M'Jid, T. Darmanin, G. Godeau, F. Guittard. *J. Mater. Chem. A* **4**, 17308 (2016).
[20] J. Bruzaud, J. Tarrade, E. Celia, T. Darmanin, E. Taffin de Givenchy, F. Guittard, J-M. Herry, M. Guilbaud, M.-N. Bellon-Fontaine. *Mater. Sci. Eng. C* **73**, 40 (2017).
[21] T. Darmanin, F. Guittard. *J. Am. Chem. Soc.* **131**, 7928 (2009).
[22] C. Mortier, T. Darmanin, F. Guittard. *Macromolecules* **48**, 5188 (2015).
[23] C. Mortier, T. Darmanin, F. Guittard. *Pure Appl. Chem.* **87**, 805 (2015).
[24] C. Mortier, T. Darmanin, F. Guittard. *Langmuir* **32**, 12476 (2016).
[25] R. M. Walczak, J. R. Reynolds. *Adv. Mater.* **18**, 1121 (2006).
[26] P. Schottland, K. Zong, C. L. Gaupp, B. C. Thompson, C. A. Thomas, I. Giurgiu, R. Hickman, K. A. Abboud, J. R. Reynolds. *Macromolecules* **33**, 7051 (2000).
[27] R. M. Walczak, J.-H. Jung, J. S., Jr., Cowart, J. R. Reynolds. *Macromolecules* **40**, 7777 (2007).
[28] A. Merz, R. Schropp, E. Doetterl. *Synthesis* **1995**, 795 (1995).
[29] G. Godeau, J. N'Na, E. El Kout, R. Ben Trad, T. Darmanin, M. El Kateb, M. Beji, F. Guittard. *Polym. Adv. Technol.* **27**, 993 (2016).
[30] G. Godeau, K. Boutet, C. Mortier, J.-P. Laugier, T. Darmanin, F. Guittard. *Mater. Des.* **114**, 116 (2017).
[31] G. Godeau, F. Guittard, T. Darmanin. *Mater. Today Commun.* **8**, 165 (2016).
[32] S. Trasatti. *Pure Appl. Chem.* **58**, 955 (1986).
[33] H. Bellanger, T. Darmanin, E. Taffin de Givenchy, F. Guittard. *RSC Adv.* **3**, 5556 (2013).